Lower Extremity Angle Measurement with Accelerometers—Error and Sensitivity Analysis

Antoon Th. M. Willemsen, Carlo Frigo, and Herman B. K. Boom, *Member, IEEE*

Abstract—Closed-loop control techniques for the restoration of locomotion of paraplegic subjects are expected to improve the quality of functional neuromuscular stimulation (FNS). We investigated the use of accelerometers for the assessment of feedback parameters. Previously, the possibility of angle assessment of the lower extremities using accelerometers, but without integration, was demonstrated. The current paper evaluates and assesses this method by an error and sensitivity analysis using healthy subject data. Of three potential error sources, the reference system, the accelerometers, and the model assumptions, the last was found to be the most important. Model calculations based on data obtained by the Elite video motion analysis system showed the rigid-body assumption error to be dominant for high frequencies (>10 Hz), with vibrations in the order of 1 mm resulting in errors of one radial or more. For low frequencies (<5 Hz), the imperfect fixation of the accelerometers combined with a nonhinge type knee joint gave an error contribution of ± 0.03 rad. The walking pattern was assumed to be two-dimensional which was shown to result in an error of ± 0.04 rad. Accelerations due to rotations of the segments could be neglected. The total error computed for low frequencies (± 0.07 rad) was comparable to the experimental difference between the current and the reference system.

INTRODUCTION

R ESTORATION of standing and walking for paraplegics can, in theory, be achieved through artificial stimulation of their neuromuscular system [1], [2]. Biomechanical instability, the delay between applied stimulus and the resulting force, variability in the stimulus-force relation, unwanted spasms or reflexes, and the essentially ballistic movements of the leg during swing are just some of the problems of FNS applications. One of the techniques investigated to improve the performance of FNS systems is artificial feedback [3]. One of the characteristics of all feedback systems is the assessment of relevant feedback parameters. In practice, this usually is at least the knee angle. Unfortunately, the development of suit-

able sensors, especially potentially implantable ones, for feedback systems has received little attention. Considering that none of the sensors presently used show a potential for implantation, we decided to investigate accelerometers for their potential as sensors in FNS systems. Accelerometers have a potential for implantation.

Previously [4], we calculated the knee angle directly, i.e., without integration, from accelerometer pairs on upper and lower leg, thereby solving the integration drift problem often associated with the use of accelerometers. For this we had to assume the movements of the lower extremities during locomotion to be two-dimensional instead of three-dimensional. Furthermore, the knee joint was modeled as a hinge joint while the lower extremity segments were treated as rigid bodies. Under these assumptions we showed the method to be successful for low frequencies with considerable errors for higher frequencies. The present study was performed to achieve a better understanding of these errors, the underlying mechanisms, and potential solutions.

THEORY

A *nonrigid* multisegment body is moving in space. The different segments are connected with three-degree of freedom ball and socket joints. A seismic accelerometer capable of measuring static accelerations is placed in the point $P_{i,j}$ (Fig. 1). Without loss of generality $P_{i,j}$ is placed on the body-fixed z-axis, connecting two consecutive joints. The equivalent acceleration which is the signal from the accelerometer including the gravitational component, is given by

$$\vec{a}_{i,j} = \vec{g} - \ddot{\vec{R}}_{i,j} \qquad (1)$$

$\vec{a}_{i,j}$: equivalent acceleration at point $P_{i,j}$
i: segment index
j: point index ($j = 0$: origin of segment.)
$\vec{g}$:   gravitational acceleration
$\ddot{\vec{R}}_{i,j}$: position of $P_{i,j}$ relative to the inertial reference system.

Dividing $\ddot{\vec{R}}_{i,j}$ in a part describing the acceleration of the body-fixed frame, and a part describing the acceleration
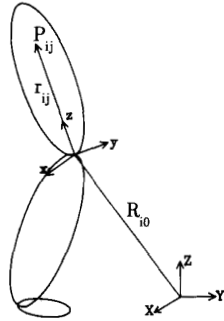
Fig. 1. Nomenclature for a multisegment body (see text). *XYZ* denotes an inertial reference system and *xyz* denotes a body-fixed system with the origin at the point of rotation, i.e., the idealized knee joint. The sagittal plane coincides with the *YZ* plane.

relative to the body-fixed frame, we obtain [5]

$$\vec{a}_{i,j} = \vec{g} - \{\ddot{\vec{R}}_{i,0} + \ddot{\vec{r}}_{i,j} + 2\vec{\omega}_i \times \dot{\vec{r}}_{i,j} + \vec{\omega}_i$$
$$\times (\vec{\omega}_i \times \vec{r}_{i,j}) + \dot{\vec{\omega}}_i \times \vec{r}_{i,j}\} \qquad (2)$$

$\vec{r}_{i,j}$: position of $P_{i,j}$ relative to body-fixed frame
$\vec{\omega}_i$: angular velocity of segment i.

To calculate the angle between two segments we use $\vec{r}_{i,j} = r_{i,j}\vec{e}_i$, with e_i the unity direction vector, and we make the *rigid-body* assumption, $\ddot{\vec{r}}_{i,j} = \dot{\vec{r}}_{i,j} = \vec{0}$. Equation (2) then reduces to

$$\vec{a}_{i,j} = \vec{g} - \ddot{\vec{R}}_{i,0} - r_{i,j}\vec{\omega}_i \times (\vec{\omega}_i \times \vec{e}_i) - r_{i,j}\dot{\vec{\omega}}_i \times \vec{e}_i.$$
$$(3)$$

Placing the body-fixed frame origins of segment i and $i + 1$ at the joint assumed to be a perfect hinge and to connect the two segments, we have $P_{i,0} \equiv P_{i+1,0}$. Consequently,

$$\vec{a}_{i,0} = \vec{a}_{i+1,0} \qquad (4)$$

where $\vec{a}_{i,0}$ and $\vec{a}_{i+1,0}$ can be obtained from (3) after placing three-dimensional accelerometers at distances $r_{i,j}$ and $r_{i,j+1}$, resulting in

$$\vec{a}_{i,0} = \frac{r_{i,j+1}\vec{a}_{i,j} - r_{i,j}\vec{a}_{i,j+1}}{r_{i,j+1} - r_{i,j}}$$

$$\vec{a}_{i+1,0} = \frac{r_{i+1,j+1}\vec{a}_{i+1,j} - r_{i+1,j}\vec{a}_{i+1,j+1}}{r_{i+1,j+1} - r_{i+1,j}}. \qquad (5)$$

So the components of $\vec{a}_{i,0}$ can be calculated in segment i body-fixed frame coordinates, whereas the components of $\vec{a}_{i+1,0}$ can be calculated in segment $i + 1$ body-fixed frame coordinates. Transforming one side of (4) to the coordinate system of the other side of the equation by multiplication with a proper rotation matrix results in three equations (one for each direction) from which the rotational angles could be solved. The advantage of this method is the avoidance of integration. However, for the lower extremities the practical implication of having to

place both accelerometers on the line connecting the joints would be to insert them in the central axis of bones. Practically, this will be extremely problematic. Fortunately, leg motion during normal walking is nearly two-dimensional. The current practice accordingly is to use this approximation, reducing (2) to

$$a_{i,j}^y = -g \sin(\theta_i) - \{\cos(\theta_i)\ddot{Y}_{i,0}$$
$$+ \sin(\theta_i)\ddot{Z}_{i,0} - 2\omega_i\dot{r}_{i,j} - r_{i,j}\dot{\omega}_i\} \qquad (6a)$$

$$a_{i,j}^z = -g \cos(\theta_i) - \{\sin(\theta_i)\ddot{Y}_{i,0}$$
$$+ \cos(\theta_i)\ddot{Z}_{i,0} + \dot{r}_{i,j} - r_{i,j}\omega_i^2\} \qquad (6b)$$

with $Y_{i,0}$ and $Z_{i,0}$ the Y and Z components of $R_{i,0}$, respectively.

Equation (4) then reduces to

$$\cos(\theta_i)a_{i,0}^y - \sin(\theta_i)a_{i,0}^z$$
$$= \cos(\theta_{i+1})a_{i+1,0}^y - \sin(\theta_{i+1})a_{i+1,0}^z \qquad (7a)$$

$$\sin(\theta_i)a_{i,0}^y - \cos(\theta_i)a_{i,0}^z$$
$$= \sin(\theta_{i+1})a_{i+1,0}^y - \cos(\theta_{i+1})a_{i+1,0}^z \qquad (7b)$$

This can be solved for $\tan(\theta_{i+1} - \theta_i)$ to give [4]

$$\tan(\theta_{i+1} - \theta_i) = \frac{a_{i+1,0}^y a_{i,0}^z - a_{i+1,0}^z a_{i,0}^y}{a_{i+1,0}^y a_{i,0}^y + a_{i+1,0}^z a_{i,0}^z} \qquad (8)$$

which can easily be processed in real-time. So with four uniaxial accelerometers on the foot, shank, thigh, and pelvis, giving a total of 16 accelerometers, the angle of ankle, knee, and hip joint can be calculated using (8), assuming that the leg segments behave as rigid bodies, the joints are one-degree of freedom hinge joints and that the movements are two-dimensional, i.e., in the sagittal plane only. It is evident that to calculate multiple angles, the accelerometers must be placed on the body-fixed z-axis connecting the consecutive joints as shown in Fig. 1.

From (5) and (8) it follows that the calculated knee angle is a function of eight accelerations and four distances. For small variations in either the accelerations or the distances, the resulting error in the knee angle (ψ) is

$$d\psi = \sum_{i=1}^{2} \sum_{j=1}^{2} \left\{ \left[\frac{\partial\psi}{\partial a_{i,j}^y}\right] da_{i,j}^y + \left[\frac{\partial\psi}{\partial a_{i,j}^z}\right] da_{i,j}^z \right.$$
$$\left. + \left[\frac{\partial\psi}{\partial r_{i,j}}\right] dr_{i,j} \right\}. \qquad (9)$$

The partial derivatives are sensitivity coefficients. They are derived in Appendix A. With these known, and after estimating the errors in the accelerations and distances, we can calculate the estimated mean ($\hat{\mu}_{d\psi}$) and standard deviation ($\hat{\sigma}_{d\psi}$) of the error in the knee angle. Rewriting (9) as

$$d\psi = \sum_{m=1}^{12} \epsilon_m \qquad (10)$$

it follows that [6]

$$\hat{\mu}_{d\psi} = \sum_{m=1}^{12} \hat{\mu}_{\epsilon_m} \qquad (11)$$

$$\hat{\sigma}_{d\psi}^2 = \sum_{m=1}^{12} \hat{\sigma}_{\epsilon_m}^2 + 2 \sum_{m=1}^{11} \sum_{n=m+1}^{12} \hat{\sigma}_{\epsilon_m \epsilon_n} \qquad (12)$$

where $\hat{\sigma}_{\epsilon_m \epsilon_n}$: estimator of the covariance between ϵ_m and ϵ_n. With $\rho_{\epsilon_m \epsilon_n} = \sigma_{\epsilon_m \epsilon_n} / \sigma_{\epsilon_m} \sigma_{\epsilon_n}$ the normalized correlation function ($-1 \le \rho \le 1$) [9], we find

$$\hat{\sigma}_{d\psi}^2 = \sum_{m=1}^{12} \hat{\sigma}_{\epsilon_m}^2 + 2 \sum_{m=1}^{11} \sum_{n=m+1}^{12} \hat{\rho}_{\epsilon_m \epsilon_n} \hat{\sigma}_{\epsilon_m} \hat{\sigma}_{\epsilon_n}. \qquad (13)$$

METHODS

We attached eight uniaxial accelerometers (Kyowa AS-5G) onto two PVC brackets. One bracket was connected to the lower leg and one to the upper leg of a healthy subject using Velcro straps. The brackets were placed on the imaginary line connecting the knee joint with either the ankle or hip joint. Another pair of accelerometers was attached on a smaller bracket and connected to the pelvis. On each bracket we also placed two hemispherical optical markers. We additionally placed two markers on the foot (at the heel and the fifth metatarsal head) as well as one on the ankle and knee joint giving a total of ten accelerometers and ten markers (Fig. 2). The accelerometer signals were amplified, low-pass filtered (40 Hz), and sampled at 500 Hz. From the accelerometer signals, the knee angle was computed by application of (5) substituted into (8).

For comparison, an Elite system [7] was used to measure both the positions of the optical markers and the signals from the accelerometers. The marker positions were captured with two cameras at 50 Hz. A separate program calculated the three-dimensional positions of each marker. The field of measurement was about 2.5 × 2.5 m and measurements started when all ten markers were detected by the system. Measurements stopped when one of the markers left the field of view.

Synchronization between marker data and accelerometer data acquisition was performed automatically. Measurements lasted between 1 and 2.5 s resulting in about two steps measured. To calibrate the accelerometers we performed measurements in two different static positions.

RESULTS

Comparison Between Elite and Accelerometer-Based Angle Signals

Fig. 3 shows a typical stick diagram of the results obtained with the Elite system. The markers on thigh and shank are not always on one line with the marker at the knee joint as is required by the theory. This holds especially during the last part of swing phase and the beginning of stance.

We used the Elite data to calculate the average distances between the accelerometers and the knee joint
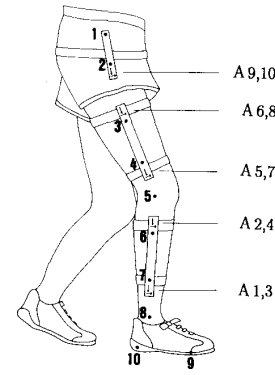

Fig. 2. Positioning of ten accelerometers, denoted by arrows and ten optical markers, denoted by dots, on the lower extremities for the simultaneous measurement of positions and accelerations. Pairs of accelerometers, one in the tangential (y) direction and one in the radial (z) direction, are placed at five sites: pelvis, two pairs at the thigh and two pairs at the shank. Accelerometers 1, 2, 5, 6, and 9 are tangential, whereas 3, 4, 7, 8, and 10 are radial. The optical markers are placed at (from top to bottom): pelvis, hip joint, two at the thigh, knee joint, two at the shank, ankle joint, fifth metatarsal, and the heel.
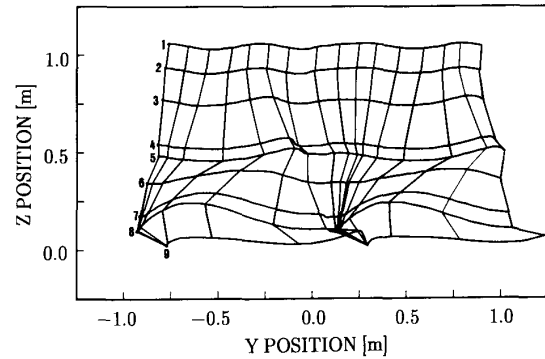

Fig. 3. Stick diagram representing the movements of the leg in the sagittal plane during walking. The optical markers are placed as shown in Fig. 2. The marker at the heel was omitted for clarity. The sequence shows one and a half step starting in the last part of the stance phase, ending just before heelstrike. Time between two consecutive frames is 0.14 s.

marker ($\overline{r_{i,j}}$) to be used in (5). A reference knee angle was calculated using the positions of the markers on the brackets and is thus independent of the measurements of the knee joint marker. The hip angle was calculated similarly, except that the two accelerometers connected to the pelvis, were assumed to be exactly at the rotational axis of the hip joint, i.e., $a_{i+1,0}^y \approx a_{i+1,1}^y$ and $a_{i+1,0}^z \approx a_{i+1,1}^z$.

Fig. 4 shows the resulting knee and hip angle data both as determined from the Elite system data and as found from the accelerometers by application of (8). These accelerometer angles are consistent with the Elite angles although deviations are clearly visible, especially during the first part of the stance phase of walking (± 1.0 s to ± 1.4 s). For the differences between the two knee angle signals we found a standard deviation $\hat{\sigma}(\Delta \psi_{knee})$ of 0.36 rad and a mean $\hat{\mu}(\Delta \psi_{knee})$ of -0.06 rad, while for the error in the hip joint angle we found $\hat{\sigma}(\Delta \psi_{hip}) = 0.29$ rad and $\hat{\mu}(\Delta \psi_{hip}) = -0.06$ rad. Additional low-pass filtering (5
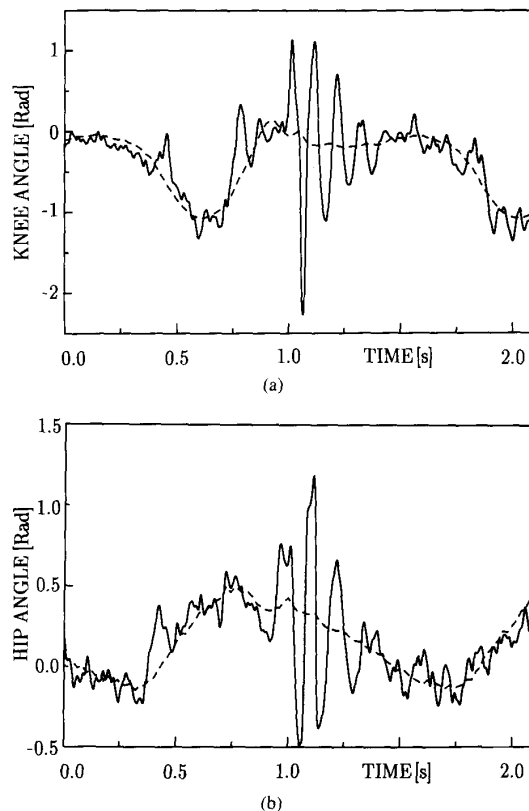
Fig. 4. Knee (a) and hip angle (b) as a function of time without filtering. Solid line—calculated from accelerations as measured by the accelerometers. Broken line—calculated from position data as measured by the Elite system.
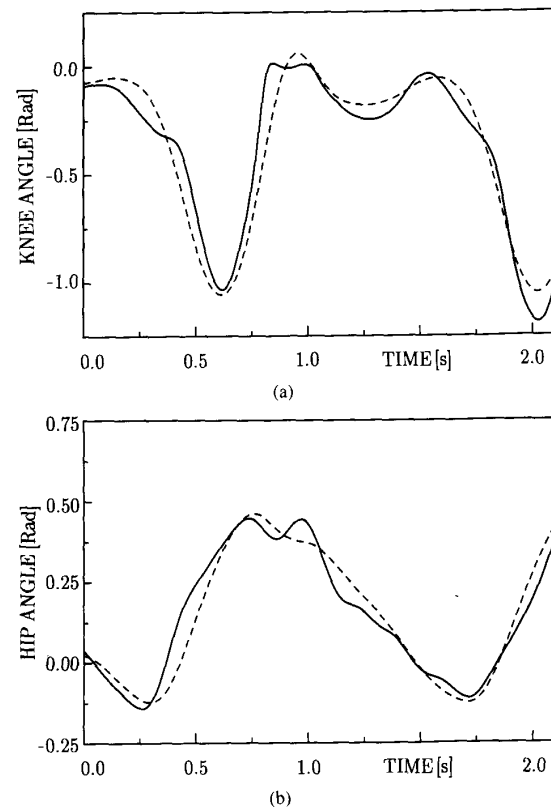

Fig. 5. Knee (a) and hip angle (b) as a function of time after filtering (5 Hz low-pass). Solid line—calculated from accelerations as measured by the accelerometers. Broken line—calculated from position data as measured by the Elite system.

Hz) diminished these errors ($\hat{\sigma}(\Delta\psi_{knee})$ = 0.10 rad, $\hat{\sigma}(\Delta\psi_{hip})$ = 0.08 rad) (Fig. 5). Taking the actual distances between accelerometers and knee joint marker to be substituted in (5), instead of the average Elite distances, reduced the standard deviation for the errors with a mere 0.01 rad.

Three potential error sources for the differences between the Elite calculated angles and those from the accelerometers are

- errors in the Elite system position data.
- errors in the measured accelerations.
- errors in the model assumptions underlying the validity of (5) and (8).

Elite System Accuracy

Accuracy of the Elite position data, using spherical markers, has been reported [7] as 1 in 2500. For a field of measurement of about 2.5×2.5 m this corresponds to ± 1 mm. We assessed this under our measurement conditions. The apparent distances between the markers rigidly connected to the brackets showed small, high frequency disturbances with standard deviations of 1.4 and 2.5 mm for upper and lower leg, respectively. These position errors are slightly higher than reported. Calculating

the angle θ_i from the positions of two markers, placed at distances of ± 0.3 m, gives an accuracy of the Elite system for angle measurements of $\pm 0.5°$. This is much smaller then the error in the angle actually found in Fig. 5. We conclude that the differences between the angle as calculated from the Elite position data and as calculated from the accelerometer data cannot be caused by errors in the Elite system position data alone.

Accelerometer Accuracy

To test our method and to estimate the accelerometer accuracy we build a mechanical double pendulum consisting of two metal bars (± 40 cm long) connected with a simple one-degree of freedom joint. A second joint was used to connect the pendulum to a rigid structure. Four one-dimensional accelerometers were connected to each segment while the "knee" angle was measured with a resolver. Using both free-swing and force movements we found the "knee" angle calculated using (8) to be accurate to 1° rad or better. We conclude that the differences between the angle as calculated from the Elite position data and as calculated from the accelerometer data cannot be caused by a lacking accuracy of the accelerometers alone.

Influence of Model Assumptions

As the differences between the Elite angle and the angle derived from the accelerometers signals, could not be explained by either the errors in the Elite position data or by errors in the accelerometer data, we have to consider that a significant part of them are caused by not fulfilling the model assumptions underlying the validity of (5) and (8). Four model assumptions made were

- the movements are in the sagittal plane and thus two-dimensional.
- the accelerometers are positioned in the central bone axis.
- the knee joint is a perfect one-axial hinge.
- the accelerometers are rigidly attached to rigid bodies.

Estimation of the effects of these assumptions on the knee angle was combined with a sensitivity analysis. The sensitivity coefficients were actually calculated from the error in the knee angle that resulted from small model induced errors in the accelerations and distances. This was performed with the aid of solely the Elite position data. To minimize the effect of differentiation noise, all position data was low-pass filtered at 5 Hz. We started with the calculation of the eight equivalent accelerations using (6). For this the angle (θ_i), angular velocity (ω_i), and angular acceleration ($\dot{\omega}_i$) of a segment were calculated from the position information of the two markers connected to the bracket. The acceleration of the knee joint ($\ddot{Y}_{i,0}$ and $\ddot{Z}_{i,0}$) was calculated from the position information of the knee joint marker. The distances r_{ij} were considered to be constant and equal to the average marker distances. The eight equivalent accelerations thus calculated from (6) as well as the distances needed in (5) received an offset of 1 m s^{-2} and 1 mm, respectively. Using (8), this resulted in a total of twelve perturbed knee angle signals, eight for the accelerations and four for the distances. Subtracting the perturbed knee angle signal from the unperturbed knee angle signal and dividing by the acceleration error (1 ms^{-2}) or distance error (1 mm) finally gave the sensitivities. They are shown in Figs. 6 and 7. This shows that the error in the knee angle is dominated by the accelerometers at the knee joint in accordance with (A14). The sensitivity for errors in the tangential accelerations is higher than for errors in the radial accelerations in accordance with (A13). The mean and standard deviation of the error in the knee angle as a function of errors in the accelerations and of errors in the distances are shown in Fig. 8. This can be used to estimate the error in the knee joint angle resulting from errors in the accelerations and distances due to the model assumptions.

To assess the effect of 3-D movements, we calculated the equivalent acceleration, expressed in inertial reference coordinates by application of (1). Then by multiplication with a rotation matrix (M_r) the body-fixed accelerations are found as

$$[a_{ij}^x, a_{ij}^y, a_{ij}^z]^T = M_r[-\ddot{X}, -\ddot{Y}, -g - \ddot{Z}]^T \qquad (14)$$
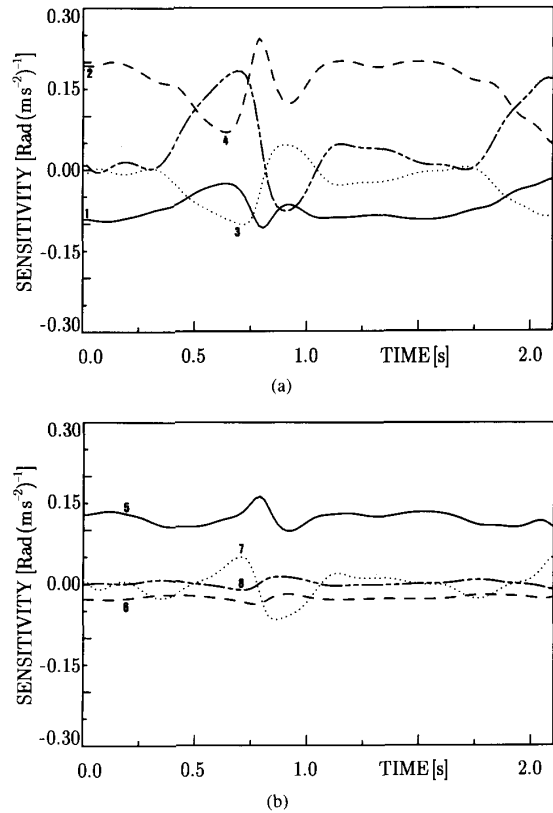

Fig. 6. Sensitivity curves of the knee angle as a function of time for constant errors in the eight accelerations (see Fig. 2) calculated from Elite position data (see text). (a) Lower leg sensitivities for errors in the accelerations. (b) Upper leg sensitivities for errors in the accelerations.
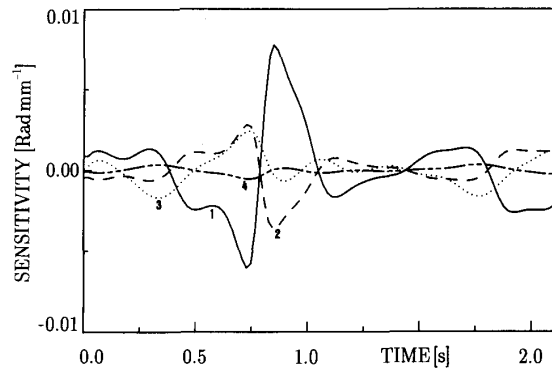

Fig. 7. Sensitivity curves of the knee angle as a function of time for constant errors in the distances from sensor to knee calculated from Elite position data (see text). 1) Distance from accelerometers 1 and 3 to knee joint. 2) Distance from accelerometers 2 and 4 to knee joint. 3) Distance from accelerometers 5 and 7 to knee joint. 4) Distance from accelerometers 6 and 8 to knee joint.

with X, Y, Z the inertial reference system coordinates of P_{ij}.

To obtain the angles not available from the Elite data, we used data from Inman *et al.* [8]. For θ_y (abduction-adduction), as well as for θ_z (internal-external rotation),
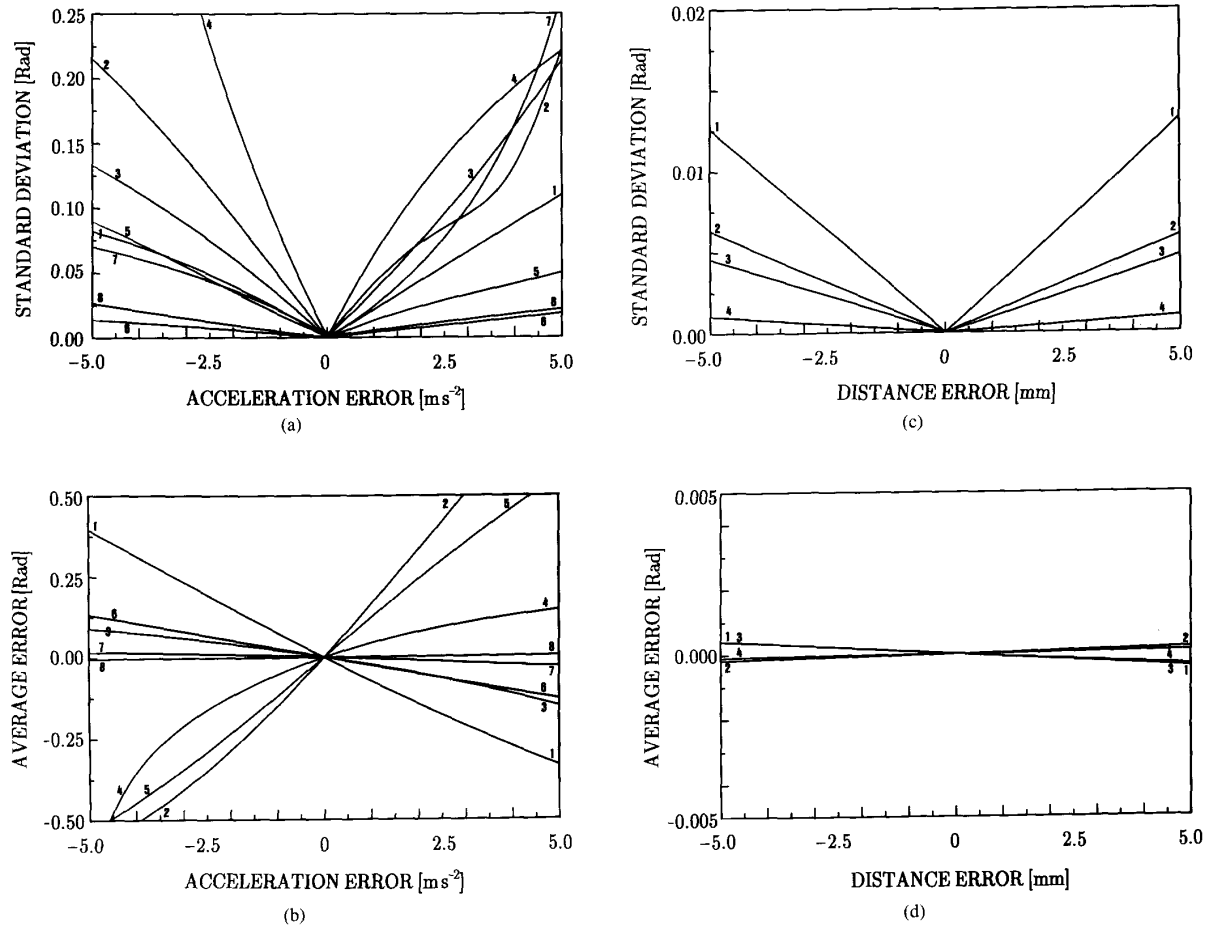
Fig. 8. Relation between constant errors in the accelerations or distances and the resulting error in the knee angle as calculated from Elite position data (see text). Numbering of accelerometers and distances as defined in Figs. 2 and 7. (a) Standard deviation of the knee angle error for errors in the accelerations. (b) Average knee angle error for different errors in the accelerations. (c) Standard deviation of the knee angle error for errors in the distances. (d) Average knee angle error for errors in the distances.

we used a worst case value of 5° for the thigh and 10° for the shank. θ_x (flexion–extension) was calculated from the Elite positions data. The rotation matrix, as a function of time, was then calculated. Comparing the accelerations then found by application of (14) with those for $\theta_y = \theta_z = 0$, resulted in errors with a standard deviation ranging from 0.04 to 0.2 ms^{-2}. This resulted in an error in the knee angle with a standard deviation of 0.04 rad.

The rotation of shank and thigh will also induce an acceleration for accelerometers not placed on the rotation axis equal to $\omega^2 r$. For accelerometers placed 0.1 m of the axis assuming a maximum rotation velocity of 1 rad s^{-1} ($\approx 60°$ s^{-1}) we find an additional acceleration of 0.1 ms^{-2}, resulting in an error with a standard deviation less than 0.01 rad. The nonideal knee joint, in combination with nonrigid-body conditions, results in a changing distance between sensors and point of rotation. The Elite data gave an average error of ± 5 mm with standard deviation less than 3 mm resulting by (5) in a knee angle error with standard deviation of less than 0.01 rad (Fig. 8). Accel-

erations are affected additionally by $+2\dot{r}_{i,j}\omega_i$ for tangential directions (6a), and $-\ddot{r}_{ij}$ for radial directions (6b). For low frequencies (≤ 5 Hz) the Elite signals thus yielded standard deviations ranging from 0.03 to 0.5 ms^{-2}, resulting in an error for the knee angle having a standard deviation of 0.03 rad.

We also looked at the effect of the nonrigid-body model assumptions for frequencies above 5 Hz. During the heel strike, as shown in Fig. 4, accelerations appeared with frequencies up to 15 Hz. If this would be generated by movements with the same frequency modeled as

$$\Delta r = A \sin (\omega t) \text{ with } \omega = 2\pi\nu, \ \nu = 15 \text{ Hz}$$

then the acceleration is given by

$$\Delta \ddot{r} = -A\omega^2 \sin (\omega t).$$

For an amplitude of 1 mm we find

$$\Delta \ddot{r} \approx 10 \text{ ms}^{-2}.$$

This is much higher than the errors we found for low frequencies or for the 3-D case. The large error in the knee angle at heel strike, as shown in Fig. 4 (± 2 rad), can be explained by a simultaneous disturbance of 2.5 mm for both the lower and upper leg segment.

CONCLUSION

The accuracy of accelerometric angle measurement at a bandwidth of 0–5 Hz, with the Elite position signals as a reference is 0.1 rad for the knee joint and 0.08 rad for the hip joint. The error in the knee angle is dominated by the accelerometers at the knee joint. The sensitivity for errors in the tangential accelerations is higher than for errors in the radial accelerations. The sensitivity for low-frequency errors in the distances is low.

Of the errors investigated, the model assumptions are the most important. Of these assumptions, the rigid-body condition is predominant. Not fulfilling this condition can explain the error in the knee angle at heel strike, as shown in Fig. 4. The use of average distances in (5) resulted in an error of 0.01 rad. Low-frequency effect of the rigid body and hinge joint condition resulted in an error of 0.03 rad. The 2-D assumptions resulted in an error of 0.04 rad. The acceleration due to rotation of the segments can be neglected. The maximal standard deviation for the error in the knee joint is found to be 0.07 rad (13).

DISCUSSION

To the best of the authors knowledge, the only alternative implantable knee angle sensor is based on Hall effect sensors. This concept was investigated by Troyk et al. [9]. They implanted two permanent magnets into the upper part of the knee joint of a dog. The Hall effect sensor was implanted in the lower part of the knee joint. A linear relation between knee angle and sensor output was obtained. Accuracy and bandwidth were not reported. This severely limits the evaluation of their concept. The distance between sensor and magnets must be small, so they have to be implanted into the joint. An advantage of this sensor is that there is no need for a mechanical connection between the two leg segments.

External fixation of the accelerometers is unlikely to fulfill the rigid-body condition. With the available techniques this restricts angle assessment from accelerometer data to low frequencies (<10 Hz). Implantation of the sensors with fixation to the skeleton may improve the rigid-body condition. The applicability of this concept, compared to the implanted Hall effect sensor also, is beyond our expertise. Even then it has to be determined which part of the high frequency oscillations seen in Fig. 4 originate from nonrigid-body properties of the knee joint.

The low-frequency result (5 Hz) from our model calculations is comparable to the error experimentally found despite the simplifications made in the sensitivity analysis. This indicates that other error sources not considered are unlikely to make a much larger contribution to the total knee angle error than the errors investigated.

The current results, both experimentally and theoretically, can be compared with preliminary data collected by Crago et al. [10] on the minimal accuracy needed for closed loop control of FNS (0.05 rad). Required bandwidth of the knee angle signal for closed loop FNS is given as 50 Hz. However, Antonsson et al. [11] showed that 99% of the signal power of the gait, as measured with a force platform, is contained below 15 Hz and 98% below 10 Hz. These frequencies should be achievable with an accelerometer system, provided that a improved fixation system can be developed. As long as external fixation of the sensors is appropriate the use of simple potentiometers is still the best choice, although far from ideal.

Finally, it has to be considered that FNS-induced walking differs significantly from normal walking. From a technical point of view this can be characterized by greater abduction and adduction of the leg, higher frequency components (roughness of the movement), and less control over heel strike. Thus, errors for FNS-induced walking are expected to be higher, while the fixation problem aggravates. Nevertheless, this study clearly shows the potential of an accelerometric angle sensor and indicates the most important error sources, i.e., not fulfilling the rigid-body and the 2-D movement condition. Control over these error sources will determine the success of our method.

APPENDIX

The sensitivity coefficients can be calculated from (5) and (8)

$$\frac{\partial \psi}{\partial a_{i,j}^y} = \frac{\partial \psi}{\partial \tan \psi} \frac{\partial \tan \psi}{\partial a_{i,j}^y} = \cos^2 \psi \frac{\partial \tan \psi}{\partial a_{i,0}^y} \frac{\partial a_{i,0}^y}{\partial a_{i,j}^y} \quad \text{(A1)}$$

$$\frac{\partial \psi}{\partial a_{i,j}^z} = \frac{\partial \psi}{\partial \tan \psi} \frac{\partial \tan \psi}{\partial a_{i,j}^z} = \cos^2 \psi \frac{\partial \tan \psi}{\partial a_{i,0}^z} \frac{\partial a_{i,0}^z}{\partial a_{i,j}^z} \quad \text{(A2)}$$

$$\frac{\partial \psi}{\partial r_{i,j}} = \frac{\partial \psi}{\partial \tan \psi_i} \frac{\partial \tan \psi}{\partial r_{i,j}}$$

$$= \cos^2 \psi \left(\frac{\partial \tan \psi}{\partial a_{i,0}^y} \frac{\partial a_{i,0}^y}{\partial r_{i,j}} + \frac{\partial \tan \psi}{\partial a_{i,0}^z} \frac{\partial a_{i,0}^z}{\partial r_{i,j}} \right). \quad \text{(A3)}$$

Realizing that for 2-D

$$(a_{i,0}^y)^2 + (a_{i,0}^z)^2 \equiv (a_{i+1,0}^y)^2 + (a_{i+1,0}^z)^2 \quad \text{(A4)}$$

we find for the first segment

$$\frac{\partial \tan \psi}{\partial a_{1,0}^y} = -\frac{(a_{1,0}^y)^2 + (a_{1,0}^z)^2}{(a_{1,0}^y a_{2,0}^y + a_{1,0}^z a_{2,0}^z)^2} a_{1,0}^z \quad \text{(A5)}$$

$$\frac{\partial \tan \psi}{\partial a_{1,0}^z} = \frac{(a_{1,0}^y)^2 + (a_{1,0}^z)^2}{(a_{1,0}^y a_{2,0}^y + a_{1,0}^z a_{2,0}^z)^2} a_{1,0}^y \quad \text{(A6)}$$

and for the second segment we find

$$\frac{\partial \tan \psi}{\partial a_{2,0}^y} = \frac{(a_{1,0}^y)^2 + (a_{1,0}^z)^2}{(a_{1,0}^y a_{2,0}^y + a_{1,0}^z a_{2,0}^z)^2} a_{2,0}^z \quad \text{(A7)}$$

$$\frac{\partial \tan \psi}{\partial a_{2,0}^z} = -\frac{(a_{1,0}^y)^2 + (a_{1,0}^z)^2}{(a_{1,0}^y a_{2,0}^y + a_{1,0}^z a_{2,0}^z)^2} a_{2,0}^y \quad \text{(A8)}$$

From (5) we find for both the y and z direction:

$$\frac{\partial a_{i,0}}{\partial a_{i,1}} = \frac{r_{i,2}}{r_{i,2} - r_{i,1}} \tag{A9}$$

$$\frac{\partial a_{i,0}}{\partial a_{i,2}} = -\frac{r_{i,1}}{r_{i,2} - r_{i,1}} \tag{A10}$$

$$\frac{\partial a_{i,0}}{\partial r_{i,1}} = -\frac{r_{i,2}(a_{i,2} - a_{i,1})}{(r_{i,2} - r_{i,1})^2} \tag{A11}$$

$$\frac{\partial a_{i,0}}{\partial r_{i,2}} = \frac{r_{i,1}(a_{i,2} - a_{i,1})}{(r_{i,2} - r_{i,1})^2}. \tag{A12}$$

Dividing (A1) by (A2)

$$\left.\frac{\partial a_{i,j}^z}{\partial a_{i,j}^y}\right|_{\partial\psi} = -\frac{a_{i,0}^z}{a_{i,0}^y} \tag{A13}$$

showing the sensitivities for errors in the accelerations at $P_{i,j}$ to be larger in the y direction than in the z direction since $a_{i,0}^z$ has an offset of 1 g. Comparing sensitivities at $P_{i,j}$ and $P_{i,j+1}$, (A1) and (A2) give

$$\left.\frac{\partial a_{i,j}}{\partial a_{i,j+1}}\right|_{\partial\psi} = -\frac{r_{i,j}}{r_{i,j+1}} \tag{A14}$$

showing the sensitivity for errors in the accelerations to be larger close to the knee joint. The same relation for errors in the distances can be derived from (A3).

REFERENCES

[1] A. R. Kralj and T. Bajd, Functional Electrical Stimulation: Standing and Walking After Spinal Cord Injury. Boca Raton, Fl: CRC Press, 1989.
[2] "Special issue on functional electrical stimulation," IEEE Trans. Biomed. Eng., vol. 36, 1989.
[3] H. J. Chizeck, R. Kobetic, E. B. Marsolais, J. J. Abbas, I. H. Donner, and E. Symon, "Control of functional neuromusculair stimulation systems for standing and locomotion in paraplegics," Proc. IEEE, vol. 76, pp. 1155-1165, 1988.
[4] A. T. M. Willemsen, J. A. van Alsté, and H. B. K. Boom, "Real-time gait assessment utilizing a new way of accelerometry," J. Biomechan., vol. 23, pp. 859-863, 1990.
[5] K. R. Symon, Mechanics. Reading, MA: Addison-Wesley, 1973.
[6] W. Feller, An Introduction to Probability Theory and its Applications. New York: Wiley, 1970, ch. 9.
[7] G. Ferrigno and A. Pedotti, "ELITE: A digital dedicated hardware system for movement analysis via real-time TV signal processing," IEEE Trans. Biomed. Eng., vol. BME-32, pp. 943-950, 1985.
[8] V. T. Inman, H. J. Ralston, and F. Todd, Human Walking. Baltimore, MD: Williams & Wilkins, 1981.
[9] P. R. Troyk, R. J. Jaeger, M. Haklin, J. Poyezdale, and T. Bajzek, "Design and implementation of an implantable goniometer," IEEE Trans. Biomed. Eng., vol. BME-33, pp. 215-222, 1986.
[10] P. E. Crago, H. J. Chizeck, M. R. Neuman, and F. T. Hambrecht, "Sensors for use with functional neuromuscular stimulation," IEEE Trans. Biomed. Eng., vol. BME-33, pp. 256-268, 1986.
[11] E. K. Antonsson and R. W. Mann, "The frequency content of gait," J. Biomechan., vol. 18, pp. 39-47, 1985.
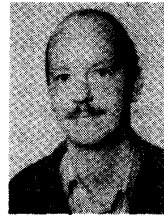
Antoon Th. M. Willemsen received the M.Sc. and Ph.D, degrees in applied physics from the University of Twente, The Netherlands, in 1984 and 1990, respectively.

In 1985 he joined the Biomedical Engineering Division of the Department of Electrical Engineering, University of Twente, working in the field of functional neuromuscular stimulation for the rehabilitation of spinal cord injured patients. His research interest are sensor for gait assessment, specifically the applicability of accelerometers, on which he wrote his dissertation—accelerometers for gait assessment in functional neuromuscular stimulation.

Carlo Frigo was born in Cittiglio (Varese), Italy, on August 3, 1952. He received the doctoral degree in mechanical engineering (bioengineering-biological control systems) from the Polytechnic of Milan, Milan, Italy in 1976.

He was a bioengineering researcher with the National Research Council from 1976 to 1980 and the Department of Electronics, Polytechnic of Milan from 1981 to 1989. He joined the Department of Bioengineering of the Polytechnic of Milan in 1989 where he is presently researcher. He is also associated with the Center for the Study of Systems Theory of the National Research Council and is at present responsible for the Laboratory of Gait Analysis of the Bioengineering Center, Pro Juventute Foundation-Polytechnic of Milan. His main research activity is in the area of neuromuscular control of human locomotion, modeling, and data processing.

Herman B. K. Boom (A'89) was trained as a medical physicist at the University of Utrecht, The Netherlands, where he received the Ph.D. degree in 1971.

He joined the Department of Medical Physics and Medical Physiology where he was engaged in research in the field of cardiac mechanics and taught physiology and biophysics. Since 1976 he has held the Chair of Medical Electronics in the Department of Electrical Engineering and is Chairman of the Biomedical Engineering Division, University of Twente, The Netherlands. His research interests are cardiovascular system dynamics, bioelectricity, and rehabilitation technology.